Synthesis and Characterization of hybrid nanoparticles with silica core and polymer shell

T. R. V. Ribeiro
Centro de Quimica-Física Molecular and IN-Institute of Nanoscience and Nanotechnology, Instituto Superior Técnico, 1049-001 Lisboa, Portugal

ABSTRACT: In this work we synthesized core-shell nanoparticles with a silica core and a poly(butyl methacrylate) shell for application in photonic materials. The silica core was labeled using a perylene derivate with two etoxy silane groups (PEOS) and the polymer shell with either a phenanthrene derivate (PheBMA) or a benzophenone derivate (NBen). The silica nanoparticles were synthesized by hydrolysis and condensation of tetraethoxysilane (TEOS), with diameters between 250 and 450 nanometers. The surface of the nanoparticles was modified with 3-trimethoxysilyl propyl methacrylate (MPS) and the surface-modified particles were used as seeds in the emulsion polymerization of poly(butyl methacrylate) shell, labelled with either PheBMA or NBen. Films casted from aqueous dispersions of clean core-shell nanoparticles are flexible and contain regularly spaced silica particles of controlled size. The formation and proprieties of the films were studied by laser scanning confocal microscopy (to identify position of the PEOS labeled silica cores) and Förster resonance energy transfer (FRET) from PheBMA to NBen (to follow the interdiffusion between the particle polymer shells during film formation.

Introduction

Nanotechnology evolves a range of techniques based on physic, chemistry, biology, materials engineering and computation. Materials in the nanoscale have been the focus of strong interest in last years because of their different proprieties, providing unique applications.[1]

Hybrid materials have many advantages compared with organic or inorganic materials. Hybrid materials combine the rigidity and thermal stability of the inorganic materials with the flexibility provided by organic materials. They have applications in coatings, optic films with high refractive index and optic wave-guides.[2-5] When the inorganic component of the hybrid material is silica, the abrasion and degradation resistance of the material could increase.[6]

Silica nanoparticles can be synthesized by polymerization of silicic acids in aqueous medium, or by hydrolysis and condensation of silicon alcoxides, known as the Stöber method.[7] In this work, we used the later method to synthesize monodisperse spherical silica nanoparticles using the precursor tetraethoxy orthosilicate (TEOS).

Fluorescent nanoparticles have considerable interest as labels or sensors.[8] Well-known photostable and fluorescent nanoparticles are the quantum dots but they still have a disadvantage, the toxicity. The problem of toxicity is resolved when organic fluorescent dyes are incorporated in silica nanoparticles and provide an alternative to quantum dots. The variety of organic fluorescent dyes provides versatile fluorescent proprieties.

Perylene derivate dyes have many applications in industrial pigments and components of photonic and electronic molecular devices.[9] They are also important for biologic analysis because they emit in red region of the spectrum (less damaging and with better penetrating in tissues).

Two perylene derivates were synthesized and used in this work (Figure 1), bis(propyl)triethoxysilane perylenediimide (PEOS)[10] and N-butyl-N'-propyl triethoxysilane perylenediimide (PEOSa)[11].

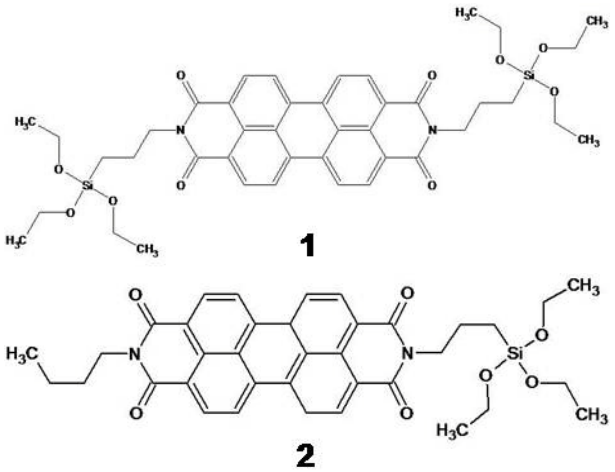

Figure 1. Structure of bis(propyl)triethoxysilane perylenediimide (PEOS, **1**) and N-butyl-N'-propyl triethoxysilane perylenediimide (PEOSa, **2**) dyes

In this work, the surface of silica nanoparticles was modified with 3-trimethoxysilyl propyl methacrylate (MPS) and the surface-modified particles were used as seeds in emulsion polymerization of polymer shell. The shell of nanoparticles labeled with either 9-phenanthryl butyl methacrylate (PheBMA, Figure 2, **3**) or 4-dimethylamino-2-acryloxy-5-methyl Benzophenone (NBen, Figure 2, **4**) was used to form flexible films studied by Förster resonance energy transfer (FRET).

The aims of this work were the study of the formation and proprieties of flexible films with nanoparticles containing silica cores. The proprieties of these films in terms of position of the PEOS labeled silica cores were studied by laser scanning confocal microscopy. During film formation, we studied the interdifusion between the particle polymer shell by FRET, using PheBMA-NBen as donor-acceptor pair.

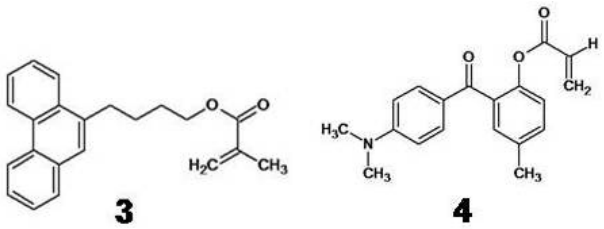

Figure 2. Structures of 9-phenanthryl butyl methacrylate (PheBMA, **3**) and 4-dimethylamino-2-acryloxy-5-methyl Benzophenone (NBen, **4**)

Experimental Section

Materials.

Absolute ethanol (Panreac, 99.5%), ammonium hydroxide solution 25% (Fluka), tetraethyl orthosilicate (TEOS, Aldrich, 98%), 3-(trimethoxysilyl)propyl methacrylate (MPS, Aldrich, 98%), sodium dodecyl sulphate (SDS, Sigma, 99%), potassium persulphate (KPS, Aldrich, 99%) were used as received. Butyl methacrylate (BMA, Sigma-Aldrich, 99%) was distilled under vacuum prior to use. Dionized water from a Millipore system Milli-Q ≥18 MΩcm were used in all synthesis steps.

4-Dimethylamino-2-acryloxy-5-methyl Benzophenone (NBen) was synthesized and characterized according to reference (1) and 9-phenanthryl butyl methacrylate (PheBMA) was synthesized according to reference (2).

Synthesis of silica nanoparticles.

Silica nanoparticles were synthesized by the Stöber Method.[7] An hydroxide ammonium solution (25%) was first added to a water/absolute ethanol mixture. When the stirred solution was stabilized at 30 ºC, TEOS was added and after stirring for 24 h, the particle dispersion was concentrated by evaporation. The resulting product was centrifuged (four cycles at 15300 rpm, 15 minutes each in a Sigma 2K15 centrifuge) and the particles were redispersed in absolute ethanol. The quantities used in synthesis are presented in Table 1.

Table 1. Reagents quantities used in silica nanoparticles synthesis by Stöber method

Synthesis	NH_4OH 25% solution	H_2O	Absolute ethanol	TEOS
	v (mL)	m (g)	m (g)	v (mL)
ST2	76.000	232.00	793.40	31.220
ST3	19.000	135.33	395.16	31.000

Synthesis of PEOS.

This dye was synthesized according to previous reference.[10] 3,4,9,10-Perylenetetracaboxylic dianhydride (0.392 g, 1 mmol) and (3-aminopropyl)triethoxysilane (1 ml, 4.3 mmol) were added to a Schlenk flask. The flask was flushed with nitrogen and stirred for 5 min. Then, the mixture was heated in an oil bath to 130 ºC for 3 h. After cooling to room temperature, the mixture was washed with petroleum ether to remove excess (3-aminopropyl)triethoxysilane. The residue was extracted using acetone/petroleum ether (1:4 v/v). After solvent evaporation, product **1** (Figure 1) was collected in needle-like red crystal form. The spectroscopic analysis was according the literature.

Synthesis of silica nanoparticles with PEOS inside.

To synthesize silica nanoparticles labeled with **1** (Figure 1), hydroxide ammonium solution (25%) was added to a water/absolute ethanol mixture. When the stirred solution has stabilized at 30 ºC, the dye was added simultaneously with TEOS. After stirring for 5 days, the particle dispersion was concentrated by solvent evaporation. The resulting product was filtered and centrifuged (four cycles at 15300 rpm for 15 minutes each, Sigma 2K15 centrifuge). The particles were redispersed in water. The quantities used in those syntheses are presented in Table 2.

Table 2. Reagents quantities used in silica labeled nanoparticles

Synthesis	NH_4OH 25% solution	H_2O	Absolute ethanol	TEOS	PEOS	PEOS (mol) / TEOS (mol)
	v (mL)	m (g)	m (g)	v (mL)	m (g)	
STM4	15.138	36.03	158.98	6.245	0.0042	0.02 %
STM5	38.000	90.29	396.42	15.610	0.0137	0.02 %
STM6	75.700	181.04	800.60	31.200	0.0162	0.01 %
STM7	75.700	180.38	793.21	31.200	0.1121	0.10 %
STM8	75.689	181.09	792.58	49.064	0.4255	0.24 %

Synthesis of PEOSa.

To synthesize PEOSa, perylene-3,4,9,10-tetracarboxylic acid dianhydride (3 g, 7.6 mmol) was stirred in KOH solution (5%, 35 mL) for 4 h at 90 °C. After cooling to room temperature, 12.5 mL H_3PO_4 (10%) was added and stirred for 1 h at 90 °C. The precipitate formed was filtered, washed with water and dried in vacuum at 100 °C. Perylene-3,4,9,10-tetracarboxylic acid monoanhydride monopotassium carboxylate (1 g, 2.2 mmol), butylamine (11 mmol) and water (50 mL) were stirred at 0–5 °C for 4 h. After stirring the mixture at 90 °C for 2 h, potassium carbonate (25%, 12.5 mL) was added and stirred for another 1 h at 90 °C. The precipitate was collected by vacuum filtration and washed with potassium carbonate (2%). The precipitate was dissolved in KOH (3.5%, 100 mL), heated to 90 °C, kept at this

temperature for 5 min and filtered while hot. After acidification with hydrochloric acid (10%), the precipitate was collected by vacuum filtration and dried in vacuum at 100 °C. Obtained 0.3 g / 30% of N-butyl-3,4,9,10-perylene tetracarboxylic acid monoanhydride monoimide. N-butyl-3,4,9,10-perylene tetracarboxylic acid monoanhydride monoimide (0.3 g, 0.7 mmol) and 5 mL of 3-aminopropyltrietoxysilane with catalytic amount of isoquinoline were repeatedly evacuated and purged with argon and then stirred at 140 °C for 72 h. Solution was extensively washed with hexane in order to remove excess of amine and remaining precipitate was extracted with chloroform, concentrated in vacuum and purified by fast flash chromatography with chloroform/ethanol 10/1 as eluent to obtain 75 mg /17.2 % yield.

^{1}H NMR (300 MHz, $CDCl_3$): 8.56 (d, 4H, *J* = 9.0 Hz), 8.42 (d, 4H, *J* = 9.0 Hz), 4.19 (m, 4H), 3.83 (m, 6H), 1.90 (m, 2H), 1.75 (m, 2H), 1,47 (m, 2H), 1.23 (m, 9H), 1.01 (t, 3H, *J* = 8.0 Hz), 0.78 (m, 2H); ^{13}C NMR (300 MHz, $CDCl_3$): 163.3, 163.2, 134.5, 134.4, 131.3, 129.2, 126.3, 123.3, 123.2, 123.0, 58.5, 43.1, 40.5, 30.2, 21.5, 20.4, 18.3, 13.9, 8.1.

Modification of the silica nanoparticle surface with PEOSa.

To modify the silica nanoparticle surface, a solution of perylene dye (46 µL, 0.166 mmol/L) was added to emulsion of the silica particles (300 mg) in dry toluene (10 mL), and allowed to reflux for 24 h. After that time the particles were centrifuged, decanted and repeatedly washed and decanted with chloroform.

Synthesis of the methoxysilyl modified silica nanoparticles.

The coupling agent 3-trimethoxysilyl propyl methacrylate (MPS) was used to modify the silica nanoparticles surface.[14] Silica nanoparticles in ethanol were stirred at 30 ºC and then MPS was added to the mixture (40 µmol MPS/m^2 SiO_2) with a plastic syringe. The reaction proceeds for 48 h. The resulting product was centrifuged (four cycles at 15300 rpm for 15 minutes each, using a Sigma 2K15 centrifuge. The particles were redispersed in absolute ethanol and were dried in an oven at 60 ºC.

Synthesis of the polymer shell.

All particles dispersions were prepared by seeded semicontinuous emulsion polymerization. The recipes are given in Table 3. SDS was dissolved in some quantity of water. Modified silica nanoparticles were added to this solution and this mixture were purged with nitrogen in a 100 mL three-necked glass reactor fitted with a condenser and a mechanical stirrer. The dispersion was purged for 30 minutes and then heated to 80 ºC under nitrogen. The distilled monomer, with or without labeling, depending on the synthesis, KPS, SDS and the rest of the water were introduced into the reactor at a constant feed rate over 6 hours. After the addition was complete, the reaction mixture was stirred and heated for another 2 h.

Table 3. Recipes for the synthesis of polymeric shell by emulsion polymerization

Synthesis	$m_{SiO_2\text{-}MPS}$ (g)	$m_{Monomer}$ (g)	m_{H2O} (g)	m_{SDS} (g)	$m_{Initiator}$ (g)	m_{dye} (g)
TR5	1.0005	5.3640	33.3046	0.0950	0.0933	-
TR7	1.0001	3.3972	35.4074	0.1057	0.0649	-
TR10	0.9999	3.5134	34.7600	0.1023	0.0650	0.0233
TR11	1.0031	4.6443	35.0500	0.1023	0.0853	0.1035

TEM measurements.

Transmission electron microscope (model H-8100, Hitachi with a LaB6 filament) images of the silica nanoparticles and core-shell nanoparticles were obtained with an accelerator voltage of 200 kV. The freeze dried particles were dispersed in water or ethanol. One drop of dilution was placed on the grid and dried in air before observation.

Fluorescent measurements.

Fluorescence emission and excitation spectrum of silica nanoparticles with **1** inside and modified silica nanoparticles with **2** on the surface were obtained with a Spex Fluorolog F112A fluorimeter in wate dispersions and in films casted on glass slides. Spectra of **1** and **2** were also obtained in toluene solution. To clean the glass slides, these were dipped in a chromosulphuric acid solution for 1 h. The glass slides were then washed with distilled water and dipped in an EDTA solution for 20 minutes, then washed with distilled water again and kept in distilled water. The glass slides were dryed with compressed air at that moment of use.

Fluorescence intensity decay curves were obtained by the singlephoton timing technique using picosecond laser excitation at 420 nm. The system consists of a mode-locked Coherent Inova 440-10 diode laser synchronously pumping a cavity dumped Coherent 701-2 Ti:Sapphire laser using DCM, which delivers 5-6 ps pulses at a repetition rate of 460 kHz. The excitation light frequency was doubled using a BBO crystal. The fluorescence was observed at 360 nm using a polarizer at the magic angle, being the scattered light effectively eliminated by a cutoff filter. The fluorescence was selected by a Jobin-Yvon HR320 monochromator with a 100 lines/mm grating and detected by a Hamamatsu 2809U-01 microchannel plate photomultiplier. The fluorescence decay curves were analyzed by a nonlinear least-square reconvolution method based on the Marquard

algorithm. All measurements were performed at room temperature.
Films were made in a teflon device and they were dry at 30 ºC in a ventilated oven.

Laser scanning confocal fluorescence microscopy (LSCFM) imaging.

In a laser scanning confocal fluorescence microscope (Leica TCS SP5) silica nanoparticles labeled PEOS were observed on clean glass slides, using the objectives HCX PL APO CS 10x (N.A.: 0.4) dry and HCX PL APO CS 63x (N.A.: 1.4) water immersion.

Fluorescence correlation spectroscopy (FCS) measurements.

FCS correlation curves were obtained in the same LSCFM used for confocal imaging with an ISS VISTA correlator and software. The correlation curve was analyzed with the 3D-Gaussian ratio model. A HCX PL APO CS 63x (N.A.: 1.4) water immersion objective was used.

Results and Discussion

Size distribution of silica nanoparticles

The silica nanoparticles were characterized by transmission electron microscopy (Figure 3) showing very good monodispersity. Nanoparticles labeled with PEOS were also characterized by laser scanning confocal fluorescence microscopy (Figure 3). Images obtained by TEM and by confocal microscopy were binarized and analysed to measure the statistical nanoparticle diameter in order to obtain the size distribution histograms (Figure 3).

The confocal experiments also show that the particles have high fluorescence intensity and are very photostable. Confocal microscopy and TEM give similar average diameter results (Figure 3).

Figure 3. Average diameters, standard deviation by treatment of micrographs obtained by transmission electron microscopy and confocal microscopy and volume proportion of water/TEOS

	D_{TEM} (nm)	$D_{Confocal}$ (nm)	H_2O/TEOS (v/v)
ST2	436 ± 32	-	7.4
ST3	319 ± 30	-	4.4
STM4	323 ± 31	-	5.8
STM5	442 ± 30	393 ± 50	5.8
STM6	409 ± 39	434 ± 64	5.8
STM7	394 ± 27	447 ± 61	5.8
STM8	273 ± 22	-	3.7

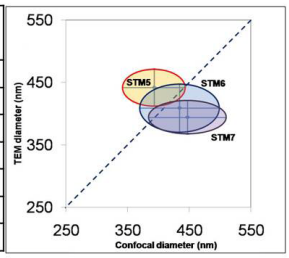

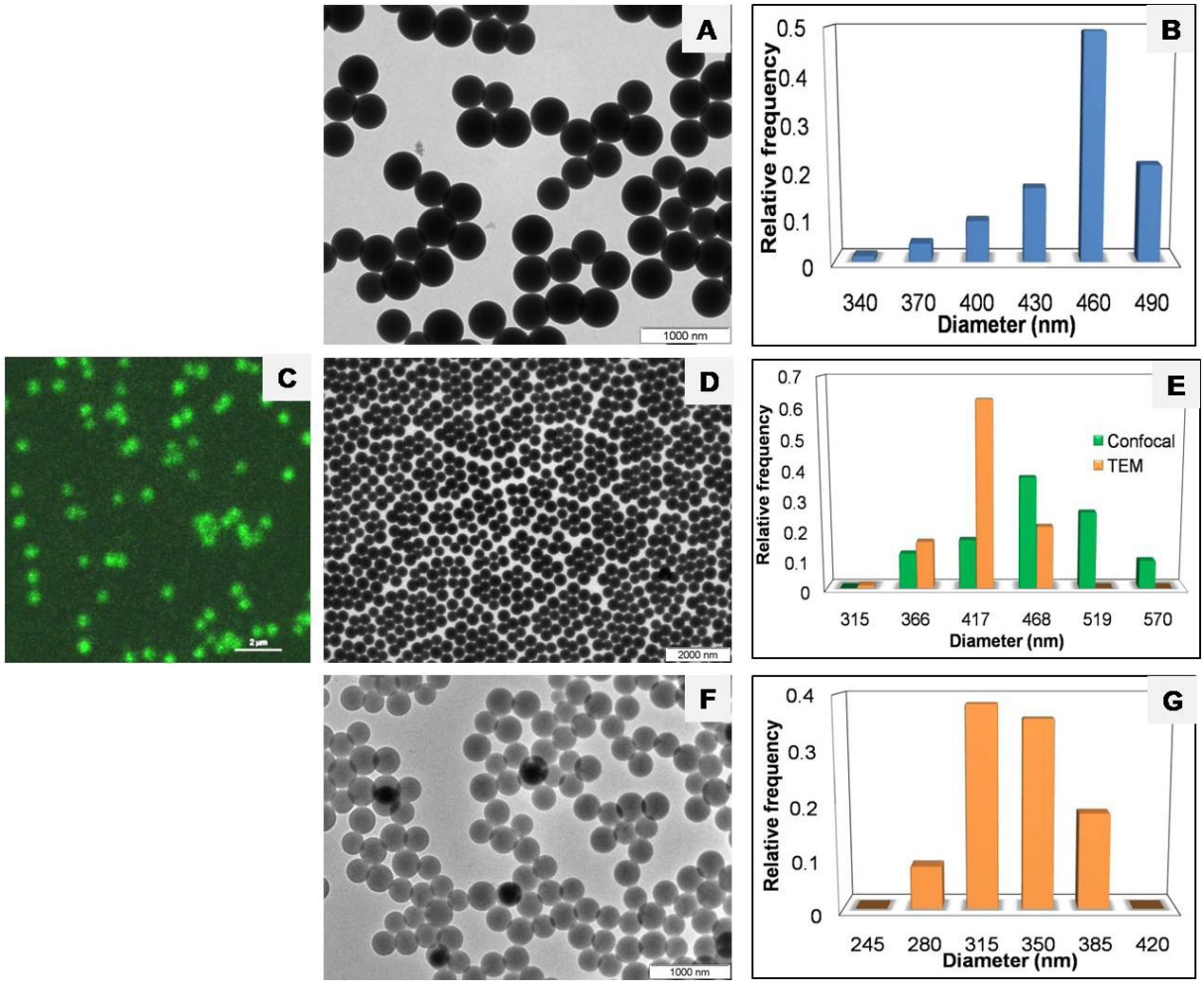

Figure 4. TEM micrographs of ST2 (A), STM7 (D) and ST3 (F), confocal image of STM7 (C) and size distributions of nanoparticles obtained by TEM (B, G, E) and confocal microscopy (E) techniques

Fluorescence of labeled silica nanoparticles

In Figure 5 A we show the fluorescence spectra of PEOS in toluene and of the silica nanoparticles labeled inside with PEOS (in film, and disperse in water and in 1,4-dioxane). The emission maximum of the nanoparticles in the film and when disperse in water suffers a deviation for higher wavelengths compared to the emission maximum of PEOS in toluene and in the nanoparticles disperse in 1,4-dioxane. These results showed that the solvent penetrates the particles affecting the emission maximum of the dye according to the solvent polarity. This is a clear indication that the silica nanoparticles are porous. In water, the emission maximum of PEOS suffers a solvatochromic deviation to higher wavelengths, because of the higher stabilization of the S_1 excited state compared to the S_0 ground state in polar solvents. The decrease in energy observed in polar solvents means that the dipolar moment of PEOS is larger in the excited state. When the particles are disperse in 1,4-dioxane (non polar solvent), there's a higher stabilization of S_0 state compared to S_1 state of PEOS, increasing the energy variation between the two states. So, we can observe a deviation to lower wavelengths of the nanoparticle emission in 1,4-dioxane, as compared to the emission in water. The spectra of 1,4-dioxane particle dispersion is similar to the spectra of PEOS in toluene due to the similarity in solvent polarizability. In the case of a film of the nanoparticles, since the dye is located inside the particles, surrounded by a polar medium (Si-O-Si bonds), a solvatochromic deviation occurred similar to the one occurred for nanoparticles disperse in water.

The same analysis was done for nanoparticles modified at the surface with PEOSa and for PEOSa in toluene (Figure 5, B). In this case, since the dye molecules are located outside the particles, and therefore they are surrounded by a non polar medium in the film and in the dioxane dispersion, no solvatochromic deviation occurred in this case.

Aggregation of PEOS and PEOSa in the particles

An usual problem in the industrial applications of perylene derived dyes is their tendency to aggregate forming dimmers or aggregates with spectroscopy properties different from the monomers. To study the possible formation of dye aggregates, we analyze the modification in the excitation spectra of PEOS labeled silica particles obtained at different wavelengths. From the excitation spectra of PEOS at different wavelengths, λ_{emi}=535, 575 and 624 nm (Figure 6), we calculate 2 ratios (Figure 6, B and C) that reveal no significant fluctuations indicating that the same species are absorbing and emitting at these wavelengths, and therefore there are no aggregates of PEOS in toluene.

We followed the same strategy for the STM6 nanoparticles measuring the excitation spectra at emission wavelengths, λ_{emi}=545, 575 and 635 nm (Figure 6, D), and calculating the spectra ratios I_{545}/I_{575} and I_{535}/I_{635}. The ratios reveal small fluctuations that suggested the presence of aggregates in the PEOS ground state, with the spectrum in black on Figure 7-B corresponding to these aggregates.

We compared the fluorescence excitation and emission spectra obtained for PEOS in toluene and for the particles STM6 dispersed in water (Figure 7, A). The spectra are quite similar, apart from the solvatochromic shift observed in the STM6 nanoparticles discussed before. After correcting for the deviation, the difference between these two spectra gives the indication of new fluorescence specie that should correspond to the emission of aggregates present in the labeled particles (Figure 7, B).

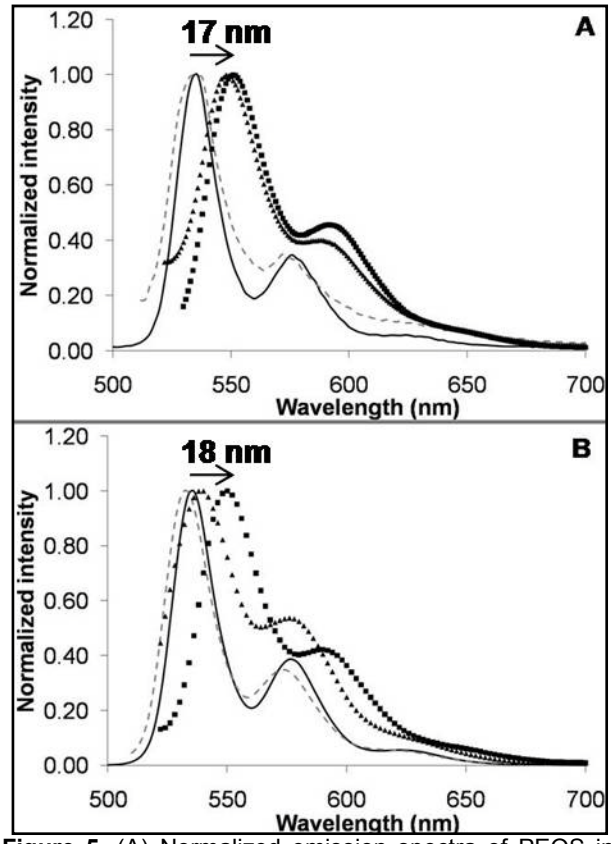

Figure 5. (A) Normalized emission spectra of PEOS in toluene (λ_{exc}=490 nm , ─), STM4 nanoparticles in film (λ_{exc}=495 nm, ▲), STM5 disperse in aqueous solution (λ_{exc}=500 nm, ■), and STM6 disperse in 1,4-dioxane (λ_{exc}=490 nm, ─ ─), evidencing a deviation of the emission maximum for higher wavelengths for nanoparticles in film and disperse in water compared to the maximum emission of PEOS in toluene and to the nanoparticles disperse in 1,4-dioxane; (B) Normalized emission spectra of PEOSa in toluene (λ_{exc}=460 nm, ─), ST3-PEOSa nanoparticles in film (λ_{exc}=470 nm, ▲), disperse in aqueous solution (λ_{exc}=470 nm, ■), and disperse in 1,4-dioxane (λ_{exc}=460 nm, ─ ─), evidencing a deviation of the emission maximum for higher wavelengths for nanoparticles disperse in water compared to the maximum emission of PEOS in toluene and of the nanoparticles in film and disperse in 1,4-dioxane

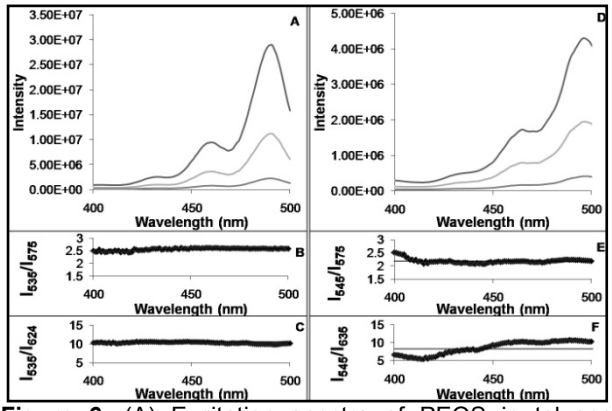

Figure 6. (A) Excitation spectra of PEOS in toluene solution obtained at λ_{emi}=535, 575 and 624 nm; (B) Ratios of the spectra obtained at λ_{emi}=535 and 575 nm (I_{535}/I_{575}) and (C) λ_{emi}=535 and 624 nm (I_{535}/I_{624}); (D) Excitation spectra of STM6 dispersed in aqueous solution obtained at λ_{emi}=545, 575 and 635 nm; (B) Ratios of the spectra obtained at λ_{emi}=545 and 575 nm (I_{545}/I_{575}) and (C) λ_{emi}=545 and 635 nm (I_{535}/I_{635})

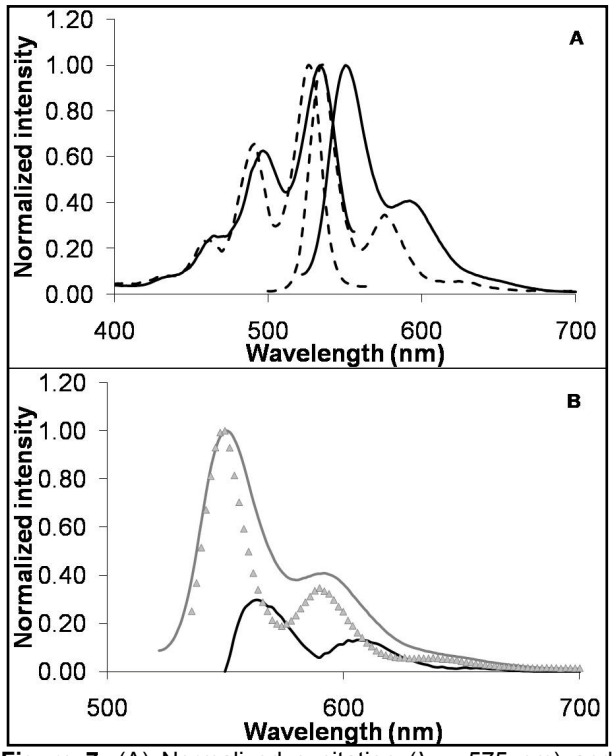

Figure 7. (A) Normalized excitation (λ_{emi}=575 nm) and emission (λ_{exc}=490 nm for PEOS in toluene and λ_{exc}=495 nm for STM6 nanoparticles in water) spectra of PEOS in toluene (- -) and of STM6 nanoparticles in water (—); (B) Normalized emission spectra of STM6 nanoparticles in water (—), and of PEOS in toluene (▲) and the difference between them (—)

The same study was made with PEOSa and ST3-PEOSa nanoparticles, showing that there is no aggregation of PEOSa in toluene (Figure 8) since the ratio of excitation spectra at different emission wavelengths are constant. For the ST3-PEOSa particles in water the ratios I_{550}/I_{590} and I_{550}/I_{650} show small fluctuations that suggested the presence of aggregates in the ground state.

The emission and excitation spectra of PEOSa are quite similar to the same of ST3-PEOSa nanoparticles, although a red shift in ST3-PEOSa nanoparticles spectrum is also observed (Figure 9, A).

Connecting the red shift and subtracting the spectra, we obtain an emission band that is attributed to the presence of emissive PEOSa aggregates in the nanoparticles (Figure 9-B). The extent of aggregation both for PEOS and for PEOSa in the silica particles is fairly small compared to other perylene derivatives.[15]

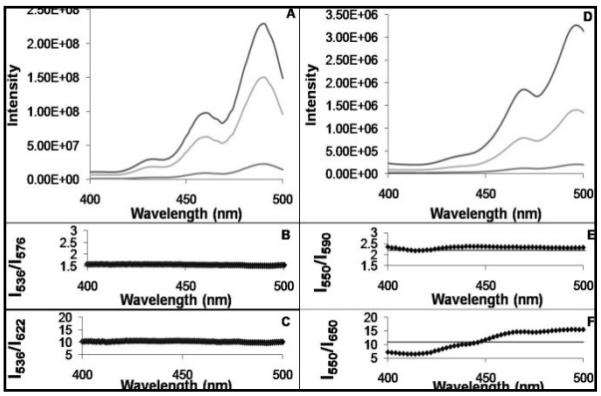

Figure 8. (A) Excitation spectra of PEOSa in toluene solution obtained at λ_{emi}=536, 576 and 622 nm; (B) Ratios of the spectra obtained at λ_{emi}=536 and 576 nm (I_{536}/I_{576}) and (C) λ_{emi}=536 and 622 nm (I_{536}/I_{622}); (D) Excitation spectra of ST3-PEOSa dispersed in aqueous solution obtained at λ_{emi}=550, 590 and 650 nm; (B) Ratios of the spectra obtained at λ_{emi}=550 and 590 nm (I_{550}/I_{590}) and (C) λ_{emi}=550 and 650 nm (I_{550}/I_{650})

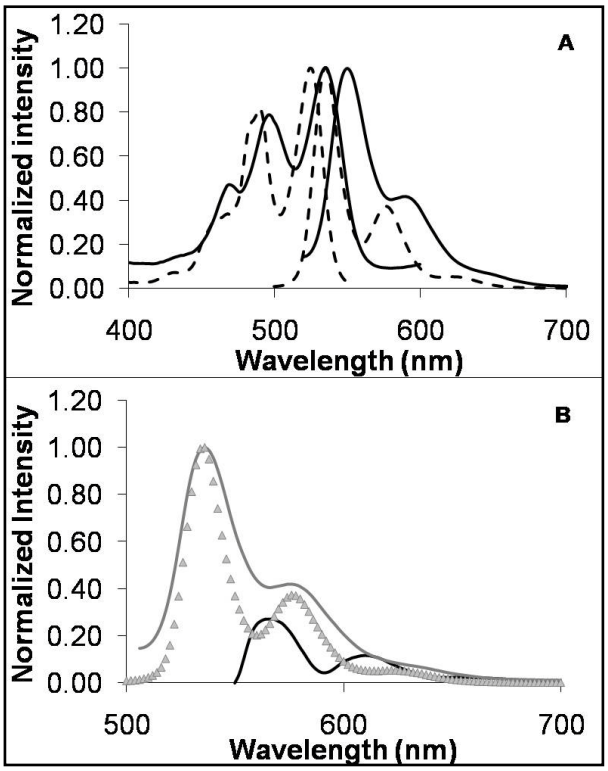

Figure 9. (A) Normalized excitation (λ_{emi}=622 nm to PEOSa solution and λ_{emi}=650 nm for ST3-PEOSa nanoparticles) and emission (λ_{exc}=460 nm to PEOSa solution and λ_{exc}=470 nm for ST3-PEOSa nanoparticles) spectra of PEOSa in toluene solution (- -) and of ST3-PEOSa nanoparticles in aqueous dispersion (—); (B) Normalized emission spectra of ST3-PEOSa

nanoparticles in aqueous dispersion (─), of PEOSa in toluene solution (▲) and the difference between them (─)

Characterization of particles with silica core and a poly(butyl methacrylate) shell

Silica nanoparticles were modified with MPS and covered with a poly(butyl methacrylate) shell via emulsion polymerization. These particles were characterized by TEM (Figure 10) but the polymer melted because of the electron beam energy. The only few particles which could be measured had ca. 950 nm of diameter, close to the expected diameter for this synthesis (1025 nm).

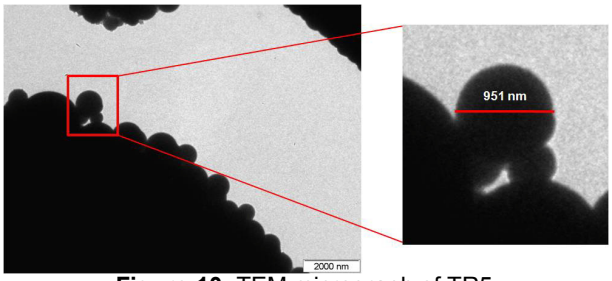

Figure 10. TEM micrograph of TR5

Since DLS did not give conclusive results for the particle size, we used fluorescence correlation spectroscopy (FCS) to measure the core-shell diameter of the particles with a PEOS labeled core. In order to evaluate the performance of this technique for measuring large particles, we started by measuring ST3 nanoparticles modified with PEOSa at the surface (ST3-PEOSa). We used STM4 nanoparticles to calibrate the system. From the TEM average diameter of these particles, we calculate the gyration radius:

$$R_g = \sqrt{\frac{3}{5}} R_{TEM} \quad (1)$$

and, since for hard spheres [16]

$$R_H = \frac{R_g}{0.775} \quad (2)$$

We calculate the particle diffusion coefficient using Stokes-Einstein equation,

$$D = \frac{k_B T}{6\pi\eta R_H} \quad (3)$$

We then fix this value in order to obtain the calibration parameter for the system. Using the w_0 value we measured the diffusion coefficient of the ST3-PEOSa nanoparticles (D=1.368 $\mu m^2/s$) and, from eq. 3 the respective hydrodynamic diameter (D_H=319 nm). The value obtained to hydrodynamic diameter by this technique was similar to the same obtained by TEM for the ST3 nanoparticles, as expected.

For long correlation times, the auto-correlation functions sow the effects of particle deposition on the substrate due to their size and high density.

For measure the diameter of the core-shell particles, we used silica nanoparticles labeled with PEOS to calibrate the system (Table 5). The hydrodynamic diameters for TR7 and TR11 obtained using eq. 3 were very close to the values expected by mass balance for the synthesis.

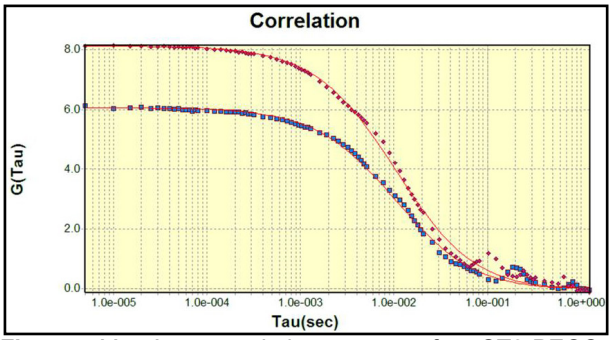

Figure 11. Auto-correlation curves for ST3-PEOSa nanoparticles, fixing w_0=0.241 obtained for STM4 nanoparticles, obtaining D=1.368 $\mu m^2/s$ by global fitting of these two auto-correlation curves

Table 4. Diffusion coefficients and hydrodynamic diameters obtained for TR7 and TR11 and the diameter expected for the mass balance of the synthesis

	Diffusion coefficient ($\mu m^2/s$)	D_H (nm)	$D_{calculated}$ (nm)
TR7	0.487	897	838
TR11	0.723	604	614

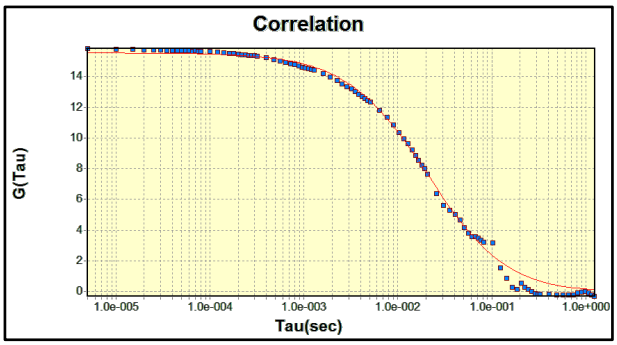

Figure 12. Auto-correlation fitting curves for TR11 by fixing w_0=0.248 obtained for STM8 nanoparticles, we obtained D=0.723 $\mu m^2/s$

Interdiffusion in polymer containing silica

When a dispersion that contains particles labeled with a donor and an acceptor dries to form a film, initially the donor and acceptor are located in different particles and energy transfer occurs only in the interface region of the particles. Annealing the film at temperatures higher than the Tg of the polymer, interdifusion of polymer chains between the particles occurs mixing donor and acceptor molecules and consequently increasing the efficiency of energy transfer (Figure 12).

We made films to study energy transfer with PheBMA/NBen as donor/acceptor pair. The silica core labeled with PEOS was used for study energy transfer using confocal microcopy. The donor and the acceptor dyes were incorporated in the polymeric shell and polymer interdiffusion was studied at two different temperatures, 60 and 90 ºC, at λ_{exc}=295 nm and λ_{emi}=350 nm.

We made 4 films in a Teflon device and the films were dried at 30 ºC in an oven. On TR10 synthesis, the polymer as labeled with NBen and on TR11 synthesis, the polymer was labeled with PheBMA.

The massic ratio of films 2 and 4 are 1:12 related to TR11:TR10 synthesis and films 1 and 3 have only particles labeled with donor. We obtained the decay curves of films 1 and 2 during the time, for 420 minutes at 60 ºC and we also obtained the decay curves of films 3 and 4 during the time, for 60 minutes at 90 ºC. We observed that the decay curves for films 1 and 3 were constant with time, which was expected due to the absence of acceptor molecules in these films. The decay curves for films 2 and 4 showed the existence of energy transfer with the increasing in time (Figure 13).

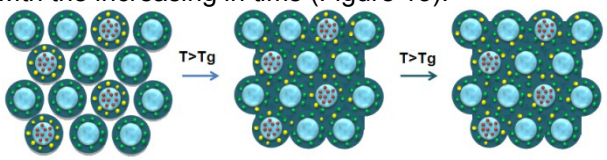

Figure 13. Representative diagram of energy transfer during the annealing time: in the beginning of the formation of the film, particles are distant occurring energy transfer only in the neighborhood, by annealing the film the polymer deforms and the mix of donors and acceptors occur, increasing the annealing time, the polymer interdiffusion increase energy transfer; in blue are represented the silica cores without PEOS, in blue with red spheres inside are represented silica cores labeled with PEOS, in green are represented NBen molecules, in yellow are represented PheBMA molecules, in dark-blue is represented the polymer

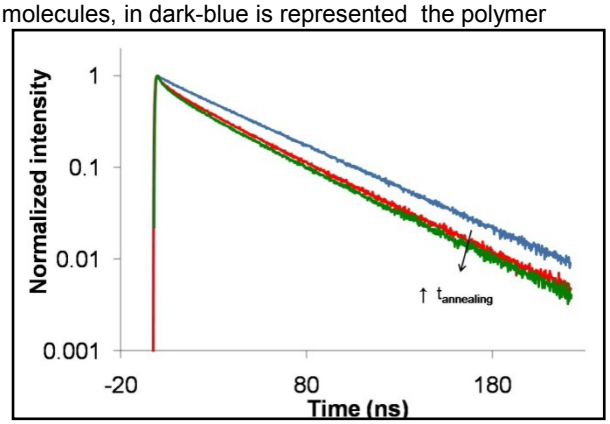

Figure 14. Fluorescence decays for film 4 at t_{annea}=15 min (red) and t_{annea}=30 min (green) at 90 ºC, in blue in both cases are the fluorescence decay of PheBMA (black arrow indicates the increase in annealing time)

Fluorescent decays areas were calculated by trapeze method and decrease with increasing on annealing time, meaning the increase in energy transfer. The energy transfer efficiency is given by:

$$\phi_{ET}(t) = 1 - \frac{\int_0^\infty I_D(t)dt}{\int_0^\infty I_D^0(t)dt} = 1 - \frac{Área\,(t_{annea})}{Área\,(D)} \qquad (4)$$

where $I_D(t)$ is the donor decay function, $I_D^0(t)$ is the donor decay in absence of acceptor, $Área(t_{annea})$ is the area under the decay curve with annealing time t_{annea} and $Área(D)$ is the area under the decay curve of the film with only particles labeled with donor molecules.

The energy transfer efficiency increases with annealing time until gets a maximum that corresponds to the maximum value of energy transfer. In this case, the maximum of energy transfer was 33%.

The apparent mixture fraction (f_m) is given by the following expression:

$$f_m \approx \frac{\phi_{ET}(t_{annea}) - \phi_{ET}(t_0)}{\phi_{ET}(t_\infty) - \phi_{ET}(t_0)} = \frac{Área\,(t_0) - Área\,(t_{annea})}{Área\,(t_0) - Área\,(t_\infty)} \qquad (5)$$

where $\phi_{ET}(t_{annea}) - \phi_{ET}(t_0)$ represents the change in ϕ_{ET} between the initially prepared film and that annealed for a time t_{annea} and $\phi_{ET}(t_\infty) - \phi_{ET}(t_0)$ represents the maximum change in FRET efficiency, between the initially prepared film and the fully mixed film.

The apparent mixture fraction increases with annealing time getting different values for the films 2 and 4. At higher annealing temperature, polymer chains diffuse more quickly and get high value for mixture fraction. The maximum value obtained for f_m was 33% for film 4 (Figure 15).

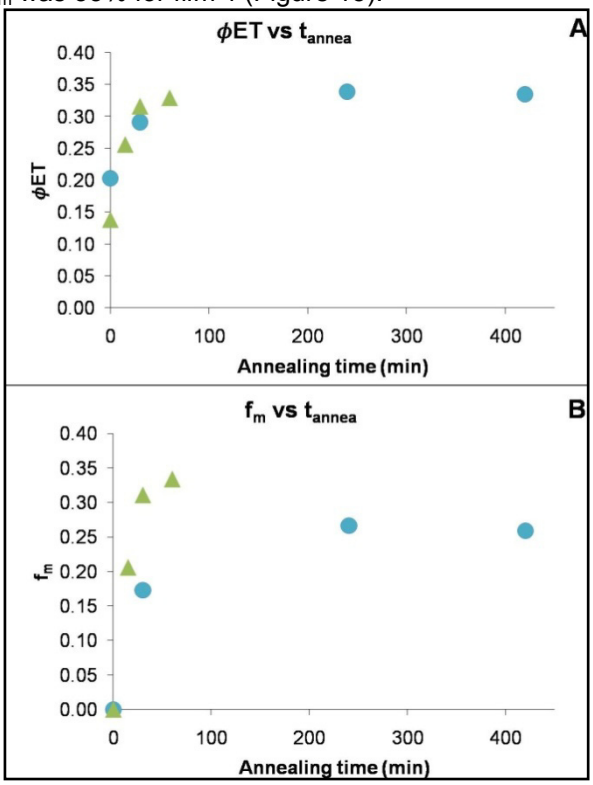

Figure 15. Graphic representation of efficiency energy transfer (A) and mixture fraction (B) for films 2 and 4 evidencing the increase of these values with annealing time

An example of these films was made from TR11 synthesis after 60 minutes of annealing at 90 ºC (Figure 16), it shows proprieties of resistance, transparence and flexibility.

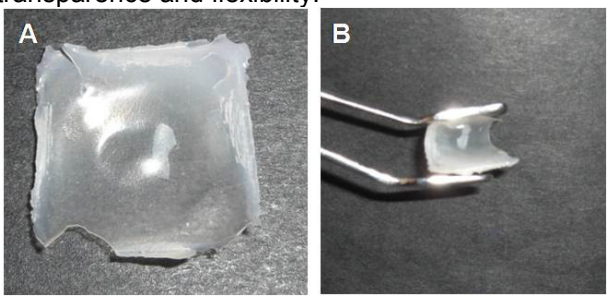

Figure 16. Images of TR11 film made in a template of teflon after 60 minutes of annealing at 90 ºC, showing proprieties of transparency (A) and flexibility (B)

Conclusions

Silica nanoparticles labeled and unlabeled were synthesized with high monodispersity proved by TEM and confocal microscope images. The dimensions of the particles obtained by TEM and confocal microscopy were similar. We conclude that silica nanoparticles labeled with PEOS are porous, comparing the emission spectra obtained to these nanoparticles in film, in water, in 1,4-dioxane and the emission spectrum of PEOS in toluene. The diameter of nanoparticles modified in the surface with PEOSa was determined by FCS and are quite similar to the diameter of these unlabeled nanoparticles obtained by TEM. Silica nanoparticles were modified in the surface with MPS to covalently link the polymer to the silica surface. Polymeric shell was covalently linked to silica cores labeled with PEOS and unlabeled. The diameter of the core-shell nanoparticles was obtained by FCS and was very similar to the values expected by mass balance. We made studies of energy transfer in films with the hybrid nanoparticles using PheBMA-NBen donor-acceptor pair and the maximum energy transfer obtained was 33% and the maximum of fraction of mixture was around 30%. These studies indicated that exist polymer interdiffusion and malleable films were obtained with silica cores distributed inside.

Acknowledgements

We acknowledged Dr. Carlos Baleizão and Marek Kluciar for the preparation of PEOS and PEOSa, Prof. Carlos Afonso for the preparation of PheBMA, and Leila Moura and Prof. Carlos Afonso for the preparation of NBen. We also acknowledge Eng. Isabel Nogueira for the TEM micrographs and Dr. Aleksander Fedorov for the fluorescence decay measurements.

Bibliograhy

(1) Zou, H., Wu, S. and Shen, J., *Chemical Review,* **2008**, *108*, 3893-3957;
(2) Ershad–Langroudi, A., et al., *Journal of Applied Polymer Science,* **1997**, *65*, 2387–2393;
(3) Papadimitrakopoulos, F., Wisniecki, P. and Bhagwagar, D. E., *Chemistry of Materials,* **1997**, *9*, 2928-2933;
(4) Wang, B., et al. *Macromolecules,***1991**, *24*, 3449-3450;
(5) Yoshida, M. and Prasad, P. N., *Chemistry of Materials,***1996**, *8*, 235-241;
(6) Sangermano, M., et al., *Progress in Organic Coatings,* **2005**, *54*, 134–138;
(7) Stöber, W., Fink, A. and Bohn, E., *Journal of colloid and interface science,* 1968, 26, 62-69;
(8) Sokolov, I. and Naik, S., *small,* **2008**, *4*, 934–939;
(9) Leroy-Lhez, S., et al., *C. R. Chimie,* **2006**, *9*, 240-246;
(10) Luo, Y. and Lin, J., *Journal of Colloid and Interface Science,* **2006**, *297*, 625–630;
(11) Pasaogullari, N., Icil, H. and Demuth, M., *Dyes and Pigments,* **2006**, *69*, 118-127;
(12) Oh, J. K., et a**l., *J**ournal of Polymer Science: Part A: Polymer Chemistry,* **2002**, *40*, 3001-3011;
(13) Afonso, C. A. M. and Farinha, J. P. S., *J. Chem. Research,* **2002**, 2-4;
(14) Liu, X., et al., *Journal of Macromolecular Science, Part A.,* **2006**, *43*, 1757-1764;
(15) Moffitt, M., Farinha, J .P. S. and Winnik, M.A., *Macromolecules,* **1999**, *32*, 4895-4904;
(16) Schärtl, W., *Light Scattering from Polymer Solutions and Nanoparticle Dispersions,* 1ª. s.l. : Springer, 2007.